Modeling study on the air quality impacts from emission reductions and atypical meteorological conditions during the 2008 Beijing Olympics

Jia Xing [a,b], Yang Zhang [b], Shuxiao Wang [a], Xiaohuan Liu [c], Shuhui Cheng [c], Qiang Zhang [d], Yaosheng Chen [b], David G. Streets [d], Carey Jang [e], Jiming Hao [a,*], Wenxing Wang [c]

[a] Department of Environmental Science and Engineering, and State Key Joint Laboratory of Environment Simulation and Pollution Control, Tsinghua University, Beijing 100084, China
[b] North Carolina State University, Raleigh, NC 27695, USA
[c] Shandong University, Jinan, Shandong Province 250100, PR China
[d] Argonne National Laboratory, Argonne, IL 60439, USA
[e] The U.S. Environmental Protection Agency, Research Triangle Park, NC 27711, USA

ARTICLE INFO

ABSTRACT

Understanding of the relative impacts of emission reductions and meteorological variations on air quality during the 2008 Beijing Olympics has an important policy implication. In this work, detailed process analyses and sensitivity simulations under different emission and meteorology scenarios were conducted using CMAQ and the Process Analysis tool to quantify the air quality benefits from emission reductions and meteorological variations in August 2008. The results indicate that emission-driven changes dominate surface concentration reductions of SO_2, NO_2, VOCs, daily maxima O_3 and $PM_{2.5}$ by −11% to −83%. The effect of meteorology-driven changes on species concentrations can be either ways (by −46% to 105%) at different locations. The dominant processes contributing to O_3, $PM_{2.5}$, SO_4^{2-}, NO_3^-, and secondary organic aerosol (SOA) are identified. Gas-phase chemistry is a major process for O_3 production, and PM processes are dominant sources for $PM_{2.5}$ in the planetary boundary layer (PBL). The reduced emissions weaken the source contributions of gas-phase chemistry to O_3 and those of PM processes to $PM_{2.5}$, with weaker vertical mixing processes and horizontal transport in the PBL. Compared with 2007, 2008 has a higher humidity, lower temperature and more precipitation that benefit O_3 reduction within the PBL, and a weaker vertical mixing that disbenefits reductions of all pollutants concentrations. Stronger process contributions of cloud processes (e.g., below- and in-cloud scavenging, and wet deposition) in 2008 help reduce concentrations of $PM_{2.5}$, NO_3^-, and SOA, but they (e.g., aqueous-phase chemistry) enhance surface SO_4^{2-} concentrations. Smaller process contributions of aerosol processes help reduce the concentrations of SOA and SO_4^{2-} but enhance NO_3^- and $PM_{2.5}$ in lower layers (1−6) due to the evaporation of NO_3^-. The ratios of $P_{H_2O_2}/P_{HNO_3}$ increase under the controlled simulation, indicating that the emission control actions enforced during the 2008 Olympics weakened the sensitivity of O_3 chemistry to VOC emissions in urban areas.

1. Introduction

As the capital, the political, economic and cultural center of China, and one of the megacities in the world, Beijing suffers severe deterioration of urban air quality since 1980s, due to the rapid increases of fossil fuel consumptions, active constructions, and vehicle population, as well as human population. The annual average concentrations of SO_2, NO_x, and PM_{10} were 55, 71, and 149 μg m^{-3} in 2004, respectively, which are much higher than those in the western countries (Hao et al., 2007). High concentrations of $PM_{2.5}$ and O_3 in Beijing were frequently reported during past decades (He et al., 2001; Sun et al., 2004; Zheng et al., 2005; Duan et al., 2006; Wang et al., 2006; Fu et al., 2009; Tang et al., 2009; Zhao et al., 2009).

In order to keep the promise of Green Olympic Principle and ensure air quality at a healthy level during 2008 Beijing Olympic Games, the Chinese government enforced a series of aggressive measures, starting two-month in advance, to maximally reduce the emissions of key pollutants in Beijing and surrounding areas. The daily emissions of SO_2, NO_x, PM_{10}, and anthropogenic non-methane

* Corresponding author. Tel.: +86 10 62782195; fax: +86 10 62773650.
E-mail address: hjm-den@tsinghua.edu.cn (J. Hao).

volatile organic compounds (NMVOC) were reduced by 41%, 47%, 55%, and 57%, respectively, during the Olympic Games (Wang et al., 2010a). These emission control efforts resulted in a significant improvement in air quality during 2008 Beijing Olympic Games. For example, both aerosol optical depths (AOD) and column mass concentrations of NO_2, SO_2, and CO from satellite-retrievals showed a noticeable reduction over Beijing and surrounding areas during the Olympic period (Cermak and Knutti, 2009; Mijling et al., 2009; Witte et al., 2009; Yu et al., 2010). The concentrations of O_3, CO, NO_2, SO_2 and particulate matter (PM) from ground-level monitoring sites also showed large decreases (Wang and Xie, 2009; Wang et al., 2009b,c,d; Branis and Vetvicka, 2010). Wang et al. (2009d) reported that the reduction in the emissions of ozone precursors accounted for 80% of the decrease in O_3 mixing ratios at the Miyun rural site compared with the same period in 2006 and 2007. Wang et al. (2010a) also reported that more than 60% of $PM_{2.5}$ concentration decreases can be attributed to emission reductions compared to one month ahead of Olympic Games (i.e., July 2008). On the other hand, some studies indicated that atypical meteorological conditions had a significant effect on air quality during the Olympic Games. Cermak and Knutti (2009) reported a statistically significant reduction in aerosol load in Beijing and the immediate surroundings by 11%, but attributed meteorological variability to be the main factor causing such a decrease. Wang et al. (2009b) reported that the atypical meteorological conditions accounted for 40% of the total variation in PM_{10} concentrations, which is more than the contribution of source control measures (i.e., 16%). Wang et al. (2010b) reported that the improved air quality on most of the days during the Olympics had apparent relationship with weather changes, which warrants future modeling studies to quantify the relative importance of the emission reduction and meteorology variations in affecting air quality.

Understanding of the effects of emission reductions and meteorological variations on air quality, in particular, those on the successful air quality improvement during the Olympic Games, is crucial for future control policy design for Beijing and other cities in China. O_3 and $PM_{2.5}$, as two major regional air pollutants, are affected by many factors including emissions of multi-pollutants (e.g., NO_x, VOCs, SO_2, NH_3, and primary particles), meteorological processes (e.g., atmospheric transport and cloud scavenging), and chemical reactions (e.g., photochemistry and multi-phase reactions). The intricate interactions among these processes usually cause highly non-linear responses of chemical concentrations to the changes of emissions. Process analysis (PA), as one of advanced probing tools embedded in the U.S. Environmental Protection Agency (EPA) Model-3/Community Multi-scale Air Quality (CMAQ) modeling system (Binkowski and Roselle, 2003), enables quantitative assessment on integrated rates of various processes and reactions, thereby quantifying their relative influences on key pollutants. PA has been widely used to study the fate and formation mechanisms of regional O_3 and particles (e.g., Jang et al., 1995; Zhang et al., 2005, 2009, 2010; Tonse et al., 2008; Xu et al., 2008; Wang et al., 2009a; Liu et al., 2010a,b, 2011).

Beijing Olympic Games, as a successful example of emission reduction actions that involved the whole society in a short time period, provides a good opportunity for researchers to evaluate the effectiveness of mandatory emission restrictions. Following an evaluation of the emission reductions during the Beijing Olympic Games reported by Wang et al. (2010a), we applied CMAQ-PA tool for a detailed process analysis and conducted multi-scenarios analysis on the model responses to emission reductions and variations of meteorological conditions in this work. Our objectives were to examine the influential processes and their sensitivity to the variation of emissions and meteorological conditions and estimate the effects of emissions reductions and atypical meteorological conditions on air quality improvement. The most influential processes that lead to the formation and accumulation of O_3 and PM species (e.g., sulfate (SO_4^{2-}), nitrate (NO_3^-), and secondary organic aerosol (SOA)) are identified. The ratios of the production rates of hydrogen peroxide (H_2O_2) and nitrate acid (HNO_3) ($P_{H_2O_2}/P_{HNO_3}$) combined with several other photochemical indicators are used to indicate the NO_x vs. VOC-limited O_3 chemistry in Beijing.

2. Methodology

2.1. Modeling system and process analysis

CMAQ version 4.7 with the 2005 Carbon Bond gas-phase mechanism (CB05) and the AERO5 aerosol module was used in this study. The meteorological fields were obtained using the fifth-generation National Center for Atmospheric Research (NCAR)/Pennsylvania State University (PSU) Mesoscale Model (MM5), version 3.7. Triple-nested simulations at 36-km over China, 12-km over the eastern China, and 4-km over the Beijing area, as shown in Fig. 1, are conducted for both August 2007 and August 2008. The emissions we used in this study are described in Supplementary information. The model system was described in our previous paper (Wang et al., 2010a). The model performance for 2007/2008 baseline simulation has been thoroughly evaluated and discussed in Supplementary information. As shown in Table S2, the statistics
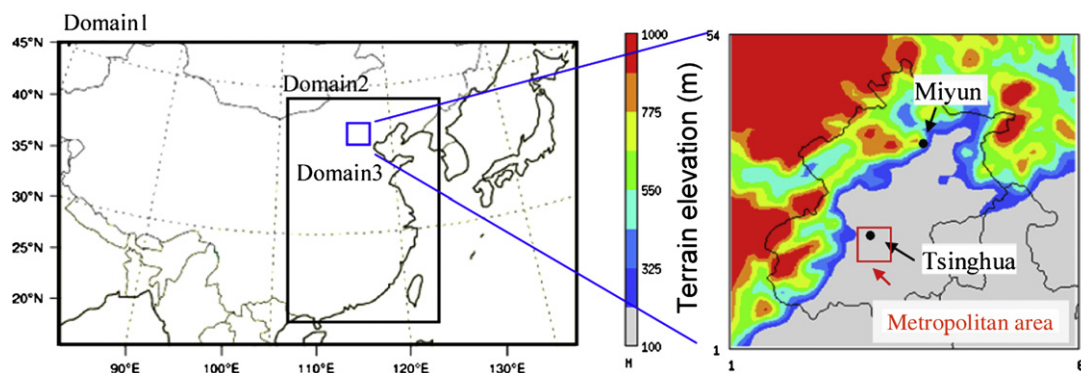

Fig. 1. Triple nesting simulation domains and locations of two observational sites: Tsinghua (THU) and Miyun (MIY) (Domain1: 36-km over China with 164 × 97 × 14 grids; Domain 2: 12-km over the eastern China with 214 × 136 × 14 grids; Domain 3: 4-km over Beijing with 54 × 60 × 14 grids. Simulation period is August 1–31, 2007 and August 1–31, 2008; THU is located in the north of metropolitan areas with millions of people and a busy on-road network. Few industry plants exist near THU. Its surrounding sources include on-road transportation and domestic emissions. It is under the influence of other sources of urban areas. MIY is a rural site, 100 km away from the Beijing urban center, and it is located in the north-west of Beijing as a direct downwind site in summer. The terrain elevation in MIY is higher than the urban area, and temperature is relative lower).

indicate that the model generally catch the meteorological conditions and pollution concentrations.

The PA in CMAQ includes the Integrated Process Rates (IPRs) and Integrated Reaction Rates (IRRs). IPRs provide hourly contributions to pollutant concentrations from seven major atmospheric processes including the emissions of primary species, horizontal transport (i.e., the sum of horizontal advection and diffusion), vertical transport (i.e., the sum of vertical advection and diffusion), gas-phase chemistry, dry deposition, cloud processes (i.e., the net effect of cloud attenuation of photolytic rates, aqueous-phase chemistry, below- and in-cloud scavenging, and wet deposition) and PM microphysical processes (i.e., the net effect of thermodynamic equilibrium and dynamics of PM species). These processes provide dominant sinks or sources of pollutants. They are identified through vertical profile analysis at various heights of PBL (defined to be the layer from the ground level to 2.9 km above the ground in this study, corresponding to the model layers of 1–10) and during different time frames (monthly-average diurnal variation analysis). The net increase or decrease in the total process contribution, calculated by summing the contributions from those processes above, indicates a net production/accumulation or destruction/depletion, respectively, of pollutant concentrations.

IRRs provide rates of 187 gas-phase reactions in CB05, which are grouped into 34 categories according to the reactions for radical initiation, propagation, production, and termination, as shown in Table 1 of Zhang et al. (2009), following the grouping approach of Liu et al. (2010b). Variables reflecting the overall tropospheric oxidation capacity include chemical production of total odd oxygen (Total_OxProd) O_x, the sum of O_3 and reactive nitrogen, as defined in Zhang et al. (2009) and the chain length of hydroxyl radical (OH) (OH_CL). From IRRs results, the ratio of $P_{HNO_3}/P_{H_2O_2}$ is used as an indicator to determine NO_x- or VOC-limited conditions for O_3 chemistry, and comparison of the amount of OH reacted with anthropogenic (OH_AVOC) and biogenic VOC (OH_BVOC) reflects the percentage of contributions from human activities and natural sources, respectively.

2.2. Simulation design and evaluation/analysis methodology

Table 1 summarizes all CMAQ-PA simulations conducted at 4-km under different emission scenarios and meteorological conditions. In addition to the 2007 baseline simulation (2007ACT) and the 2008 baseline simulation (2008ACT) for August 2007 and August 2008, respectively, two hypothetical simulations were conducted to identify the influences of emissions and meteorological conditions. Hypothetical simulation in August 2008 (2008HYP) was simulated with the 2008 meteorological conditions but the 2007 emissions that did not include mandatory emission reductions. The differences between 2008ACT and 2008HYP can provide an estimate of the effectiveness of the mandatory emission reductions during August 2008 Olympics (i.e., Emis-driven changes). Hypothetical simulation in August 2007 (2007HYP) is simulated using the 2007 meteorological conditions but the 2008 emission that considered the emission reductions. The differences between 2008ACT and 2007HYP reflect the influences from meteorological conditions (i.e., Met-driven changes). Detailed analysis was performed at THU and MIY, which represents urban and rural conditions, respectively, as shown in Fig. 1.

3. Results and discussions

3.1. Air quality responses to changes in emission and meteorology

In August 2008, it presents some atypical meteorological conditions compared to 2007. Fig. 2 compares simulated meteorological conditions in 2007 and 2008 in terms of 2-m temperature (T2), 2-m relative humidity (RH2), wind speed at 10-m (WSP10), wind direction at 10-m (WDR10), precipitation (Precip.), and PBL height (PBLH). August 2008 had higher RH (by 17.3% domainwide mean), slightly lower T (by -1.5 °C), heavier Precip. (by 12 mm month^{-1}), and lower PBLH (by 80 m). The monthly average WSP around urban areas was similar in both months, varying within 0.2 m s^{-1} in urban area. The dominant WDR was from south to the north in both months. Those comparisons indicate the possible impacts of meteorological changes in 2008 relative to 2007 on air quality. Higher RH, slightly lower T as well as heavier Precip. in 2008 will favor a cleaner air, while lower PBLH in 2008 will exaggerate air pollution. The net meteorological impacts on air quality depend on the magnitude of these competing effects.

The changes in simulated air quality in 2008, relative to those in 2007, can be attributed to both emission reductions (Emis-driven) and variations in meteorological conditions (Met-driven). As shown in Figs. 3 and 4, positive effects on pollutant concentrations reduction by Emis-driven changes are dominant for SO_2, NO_2, VOCs, O_3, and SOA domainwide. However, the extent of effectiveness of emission reductions varies spatially, due to the non-linear responses of the model predictions to complicated atmospheric physical and chemical processes. For gaseous species (see Fig. 3), the Emis-driven changes of SO_2, NO_2 and VOCs could vary from little (i.e., -0.14%, -0.15% and -0.93%, respectively) to strong impacts (i.e., -70.4%, -82.7%, and -56.3%, respectively) over the whole domain. The location of maximum reduction in SO_2 and NO_2, that occurs in the southwest of Beijing (where small boilers and cement plants used to locate before their relocations) and the reduction of VOCs is maximum over central Beijing, they are different from O_3 reduction maximum area. Monthly-averaged O_3 reduction by Emis-driven changes is more concentrated in the north of Beijing (up to -10.8%) which is located in the downwind direction of urban areas. For particles (see Fig. 4), $PM_{2.5}$ and SO_4^{2-} concentrations were reduced more by Emis-driven effects in the south (by 0 to -55% and 0 to -25%, respectively). The reduction in the concentrations of NO_3^- and SOA occurred over much larger areas, particularly in the north of Beijing following the downwind direction, which are similar to O_3. Their Emis-driven effects can

Table 1
Baseline and sensitivity simulations conducted in this study.

| Simulation short name	Model setup	Simulation description	Emission scenario
2008ACT	August 2008 at 4 km, with PA	August 2008 simulation with actual meteorology and emissions	"Actual" emissions with the reductions enforced during Olympics, considered to be 2008 baseline
2008HYP	August 2008 at 4 km, with PA	August 2008 simulation with meteorology but hypothetic emissions	"Hypothetic" emissions without reduction, the same as 2007 actual emissions
2007ACT	August 2007 at 4 km, with PA	August 2007 simulation with actual meteorology and emissions	"Actual" emissions for 2007, considered to be 2007 baseline
2007HYP	August 2007 at 4 km, with PA	August 2007 simulation with meteorology but hypothetic emissions	"Hypothetic" emissions with reductions enforced during 2008 Olympics
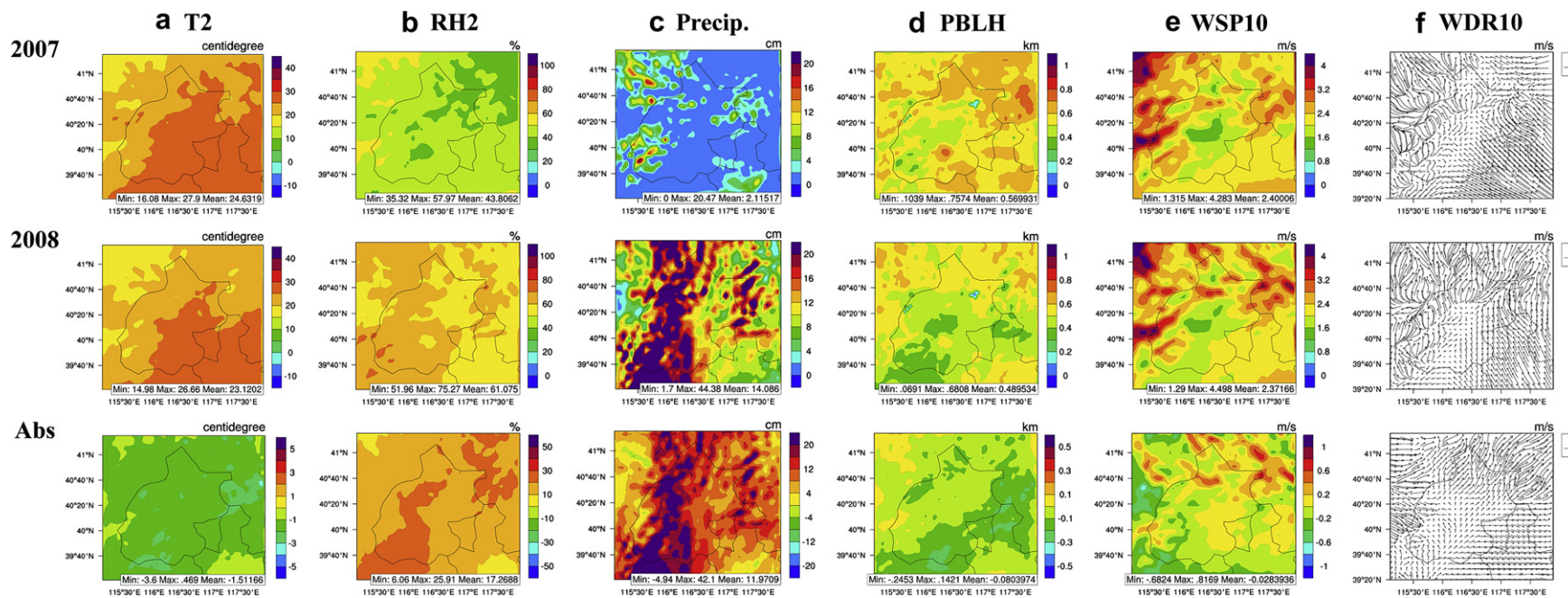
Fig. 2. Simulated meteorological conditions in August 2007 and August 2008, as well as their differences (Abs: 2008 minus 2007). Note that all variables are monthly-mean except for precipitation which is the total amount in the whole month. T2 − Temperature at 2-m; RH2 − Relative humidity at 2-m; Precip. − Precipitation; PBLH − PBL height; WSP10 − wind speed at 10-m; WDR10 − wind direction at 10-m.
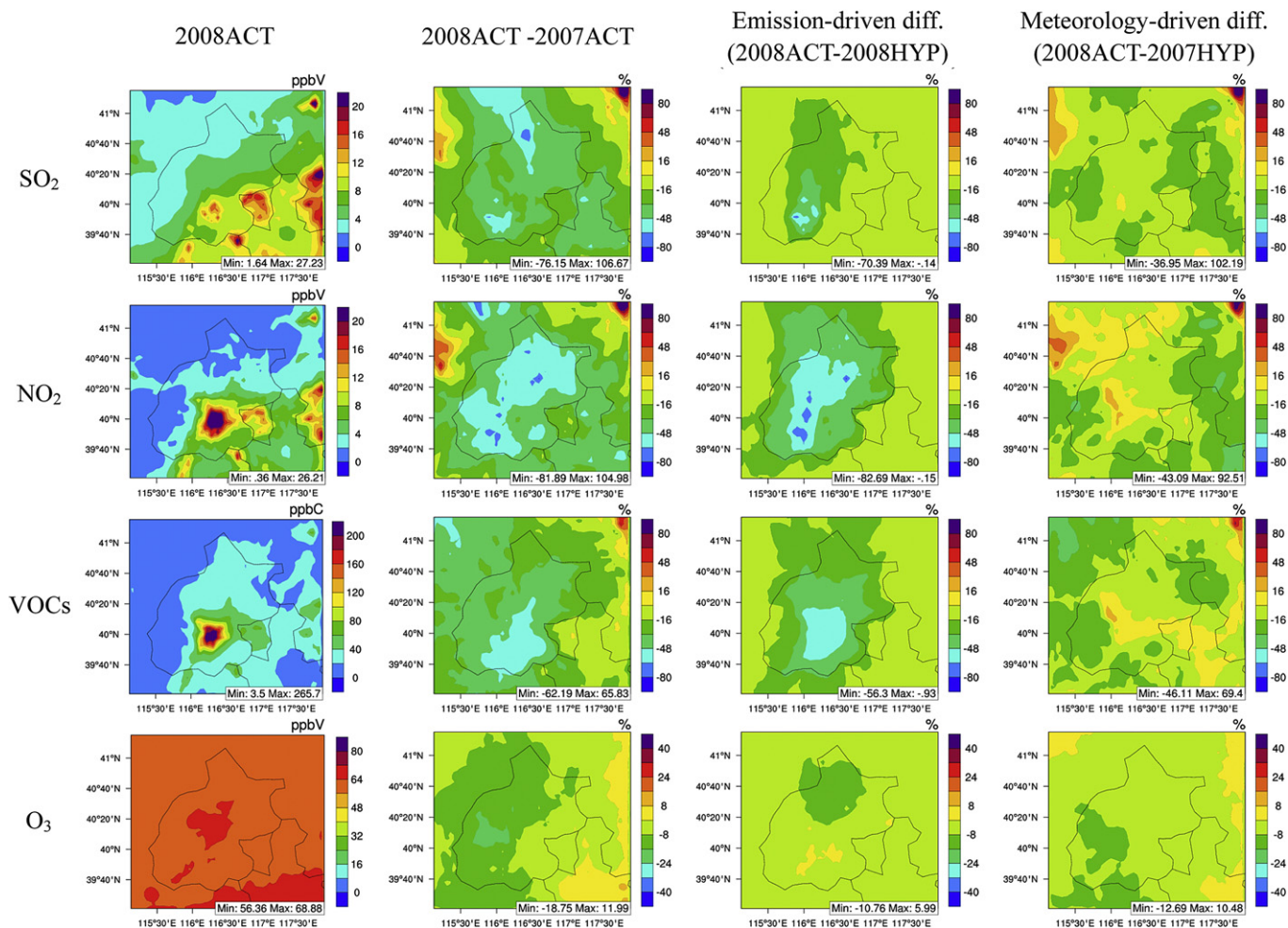
Fig. 3. Monthly-mean spatial distributions of gaseous species concentrations in August 2008ACT, the differences between 2008ACT and 2007ACT, and the net contributions of changes in emission and meteorology to such differences (all values are monthly-mean hourly concentrations except for O$_3$, which are monthly-mean of daily maximum concentrations).

cause concentration reductions by up to −28% and −11%, respectively.

The effect of Met-driven changes on species concentrations can be either ways at different locations. For SO$_2$, NO$_2$, and VOCs (see Fig. 3), positive impacts on pollutant concentration reduction (up to ∼−30%) from MET-driven changes occurred in rural area of Beijing and negative impacts (up to ∼20%) occurred around or near urban areas. Relatively lower PBLH, slightly lower WSP in 2008 (see Fig. 2d,e) inhibit dispersion of primary pollutants. This exaggerated local air pollution in urban area, and benefited air quality in downwind rural areas. Obvious negative impacts (up to ∼100%) occurred in the northeast corner of the simulated domain, caused by the stronger southwest and south to northeast flow from the polluted southeast areas in August 2008 (see Fig. 2f). Positive impact on reductions in O$_3$ mixing ratios was more concentrated in the southwest area (up to −13%). Lower temperature and higher RH favor such reductions. Dominant negative impacts are found in all PM species over most area of Beijing (except for NO$_3^-$ and SOA in some areas in the west and east portions of the domain). Impacts from Met-driven changes on PM$_{2.5}$, SO$_4^{2-}$, NO$_3^-$, and SOA are up to ∼30%, ∼60%, ∼60% and 8% in Beijing area, respectively. Domainwide higher RH in August 2008 (see Fig. 2b) favors SO$_4^{2-}$ formation in aqueous phase. Domainwide lower T and higher RHs (see Fig. 2a) in August 2008 inhibited the evaporation of NO$_3^-$ during afternoon time in polluted areas, which may dominate over a stronger

scavenging effect by more frequent precipitation domainwide (see Fig. 2c), leading to a net increase in NO$_3^-$ concentrations in polluted areas. Therefore, the impacts from Met-driven changes are negative on NO$_3^-$ reduction in polluted area and positive in the rural area, except in the northeast corner. Met-driven changes of SOA reductions are influenced by changes in its precursor as VOC responses to changes in meteorology. Similarly, strong negative impacts are found in polluted area, and positive impacts in rural areas except the northeast corner. In addition, domainwide lower T (see Fig. 2a) favors SOA formation from semi-volatile oxidation products.

3.2. Analyses of Integrated Process Rates (IPRs)

The IPR analysis can identify the dominant processes and mechanisms underlying the model responses to changes in emissions and meteorology. The responses of process contributions to such changes along with baseline IPR results are provided below.

3.2.1. IPR analysis on O$_3$ in August, 2008

Figs. 5 and 6a, b, c, d show the results of IPR from the baseline simulation 2008ACT for O$_3$, and PM$_{2.5}$, respectively, at two sites (THU and MIY). Figs. 5 and 6e, g, h compare IPR results of 2008HYP and 2008ACT. Figs. 5 and 6f show the responses of process contributions to the changes of emissions, which are obtained by taking differences in IPR results between simulations 2008HYP and
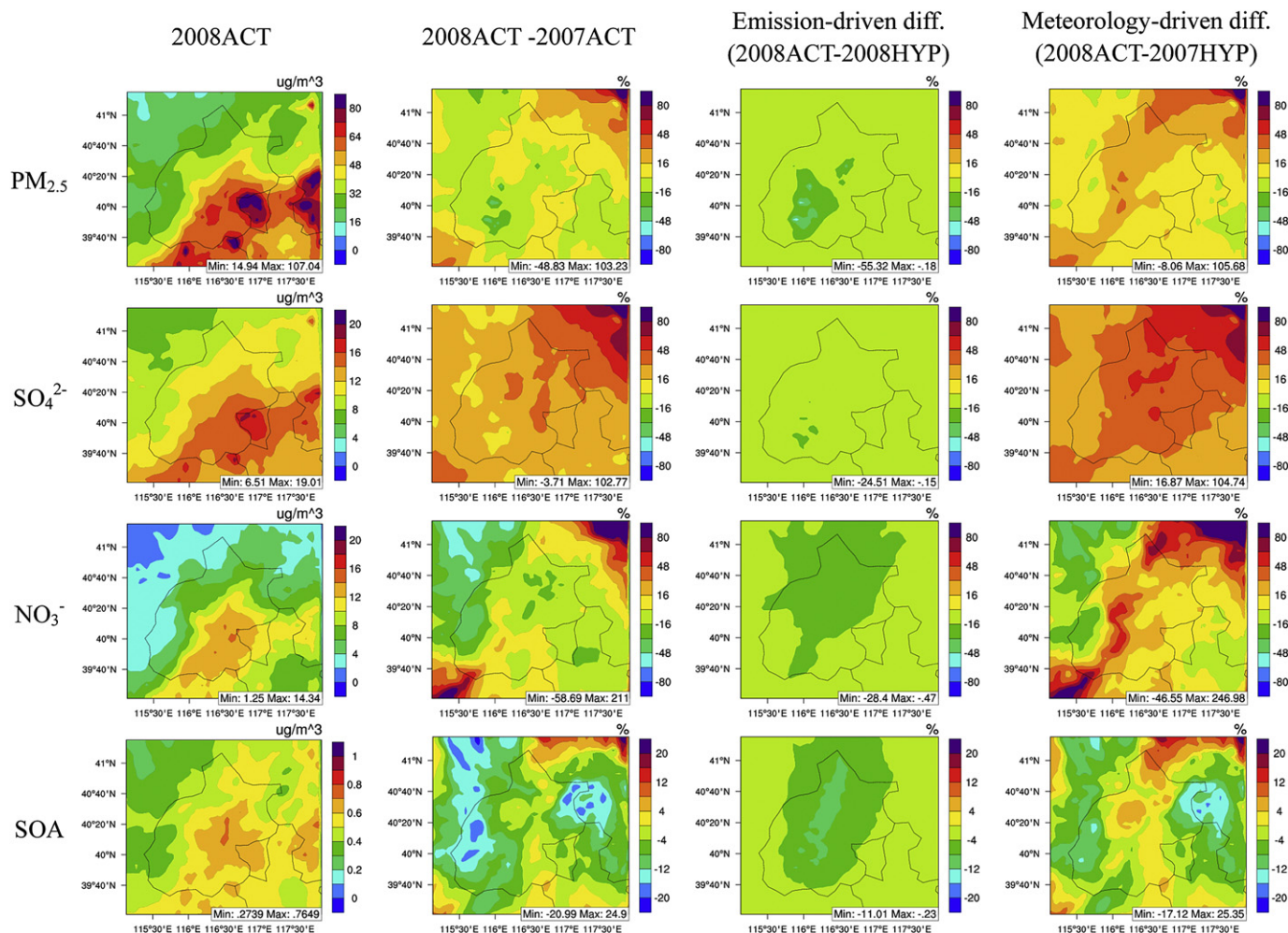
Fig. 4. Monthly-mean spatial distributions of PM species concentrations in August 2008ACT, the differences between 2008ACT and 2007ACT, and the net contributions of changes in emission and meteorology to such differences.

2008ACT. As shown in Fig. 5a, for selected afternoon hours (12:00–17:00 local time (LT)) in 2008 in the PBL, gas-phase chemistry contributes to O_3 production at both THU and MIY sites. Horizontal transport is the major sink of O_3 at THU. Horizontal and vertical transport can be either a sink or a source of O_3 at MIY, indicating the relative importance of regional transport and vertical mixing in O_3 production and accumulation at this site. Vertical profile of process contributions shown in Fig. 5b indicates that gas-phase chemistry contributes to O_3 production above the surface layer (layers 2–9) at THU. Gas-phase chemistry contributes little during afternoon time (see Fig. 5c-1) in the surface layer at THU due to sink processes including titration of O_3 by NO and termination of OH by excessive NO_2. But significant contributions from gas-phase chemistry are shown in upper layers as 2–9, during afternoon time (see Figs. 5d-1). Dry deposition acts as a major sink during afternoon when O_3 mixing ratios are high at THU. Vertical transport through mixing (by turbulence) brings high O_3 from upper layers to surface layer, contributing to the accumulation of surface O_3 mixing ratios. Controlled by dominant vertical wind direction (see the structure of vertical wind in Fig. 7, upward wind dominates in layers 1–6 and downward wind dominates in layers 7–8), the air mass in lower layers (layers 2–6) and higher layers (9–10) are blown into mid-layers (7–8) at THU, therefore the vertical transport in layers 2–6 and 9–10 acts as a major sink while in layer 7–8

acts as a major source but horizontal transport becomes a major sink. This suggests that the height of O_3 export from urban area are in layers 8–9 (1.5–2 km above ground). At MIY, downward wind dominates in layers 3–10 (the strongest downward wind speed occurs in layer 7); dominant vertical wind blows the air mass in upper layers to lower layers. Therefore, the vertical transport in layers 1–6 acts as a major source and in layers 8–10 acts as a major sink and horizontal transport becomes a major source instead. Little contributions from gas-phase chemistry are found in layers 1–7 during afternoon time (see Fig. 5b-2, c-2 and d-2). As shown in Fig. 5c-1, gas-phase chemistry acts as the major sink in urban areas during nighttime due to titration of O_3 by NO and no photochemical reactions to generate O_3. The major sink is dry deposition during the daytime for both THU and MIY sites.

Comparing the uncontrolled level during the same period (i.e., 2008HYP) to the 2008 baseline (i.e., 2008ACT), the responses of IPRs in the PBL show larger contributions of gas-phase chemistry and a stronger removal of horizontal transport at both sites (Fig. 5e). While higher precursor emissions enhance the negative impacts of gas-phase chemistry on O_3 at the urban site in lower layers (layers 1–3), they increase the source contributions of gas-phase chemistry in upper layers at the urban site and all layers at the rural site (Fig. 5f). As shown in the diurnal variations in the surface layer (Fig. 5g), the net-increase lines of O_3 show an obvious
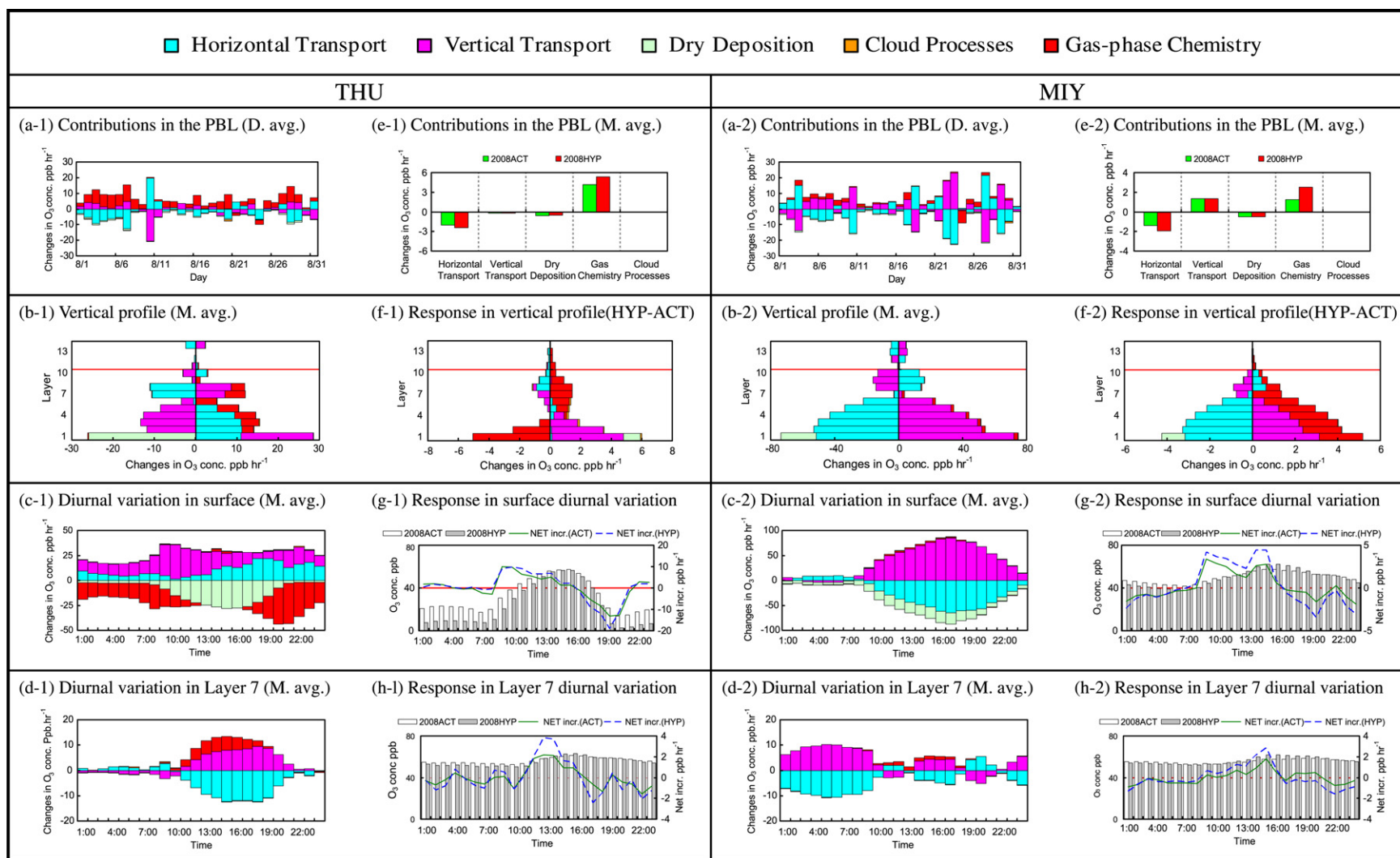
Fig. 5. Integrated processes contributions to O$_3$ mixing ratios in August 2008 (afternoon time (12:00—17:00 Local Time (LT)) for contributions in the PBL (layers 1—10) and vertical profile analysis (i.e., Figures a, b, e, f); diurnal variations are monthly-average values over 1:00 to 24:00 LT (i.e., Figures c, d, g, h); NET. Incr. is calculated by summing the contributions from all processes; M. avg. = monthly-average value; D. avg. = daily average value. The height of layers 1—10 above ground are 36, 72, 145, 294, 444, 674, 1070, 1568, 2093, and 2940 m, respectively).
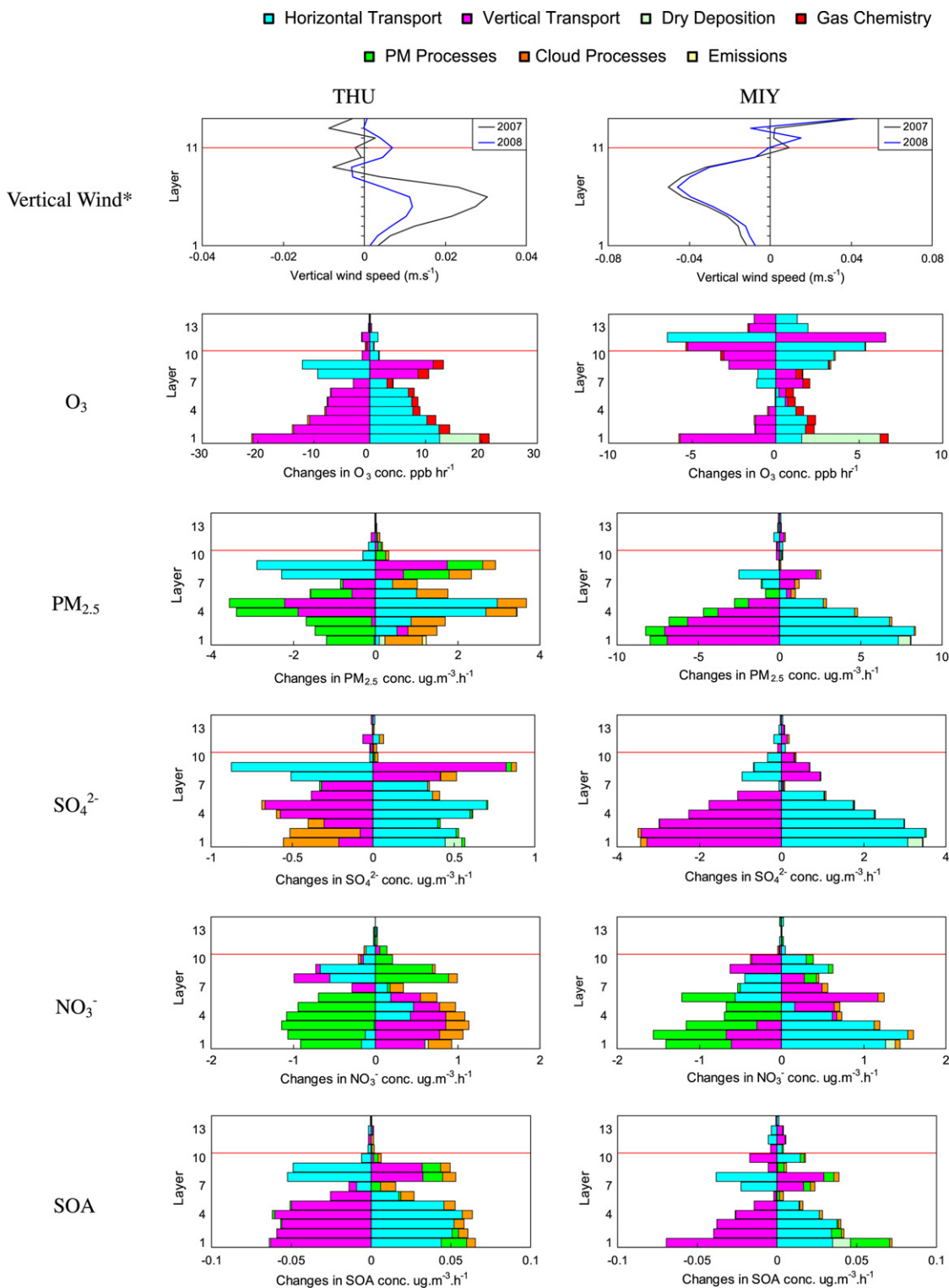
Fig. 6. Integrated processes contributions to PM$_{2.5}$ mass concentrations in August 2008 (diurnal variations are based on monthly-average values over 1:00 to 24:00 Local Time (LT); NET. Incr. is calculated by summing the contributions from all processes; M. avg. = monthly-average value; D. avg. = daily average value; The height of layers 1–10 above ground are 36, 72, 145, 294, 444, 674, 1070, 1568, 2093, 2940 m, respectively).

Fig. 7. Differences in vertical profiles of IPRs between two meteorological conditions (2007ACT minus 2008ACT, based on monthly average of values during selected afternoon time (12:00–17:00 Local time (LT)) for O₃, monthly-average values over 1:00 to 24:00 LT for other species, The heights of layers 1–10 above ground are 36, 72, 145, 294, 444, 674, 1070, 1568, 2093, 2940 m, respectively). * MIY is located at the edge of mountain areas where strongly affected by the mountain-valley wind; THU is located in the urban area, where the upward wind dominates caused by the urban heat island effect.

peak around 9–10 am at both sites, which indicates the breaking of an inversion layer with an enhanced vertical mixing. The second O₃ peak appeared at 1–2 pm at THU and at 3–4 pm at MIY, which is due to photochemical production. Obvious enhancement of net-increase lines can be found after 9–10 am (when the inversion layer

breaks down) at surface and during the peak O₃ time (1–2 pm at THU and 4 pm at MIY) in layer 7 (Fig. 5g and h). Little increase in the O₃ mixing ratios at surface at THU due to changes in NO emissions (though a slight increase appeared in upper layers,) but the O₃ reduction during nighttime is much larger, due to a stronger
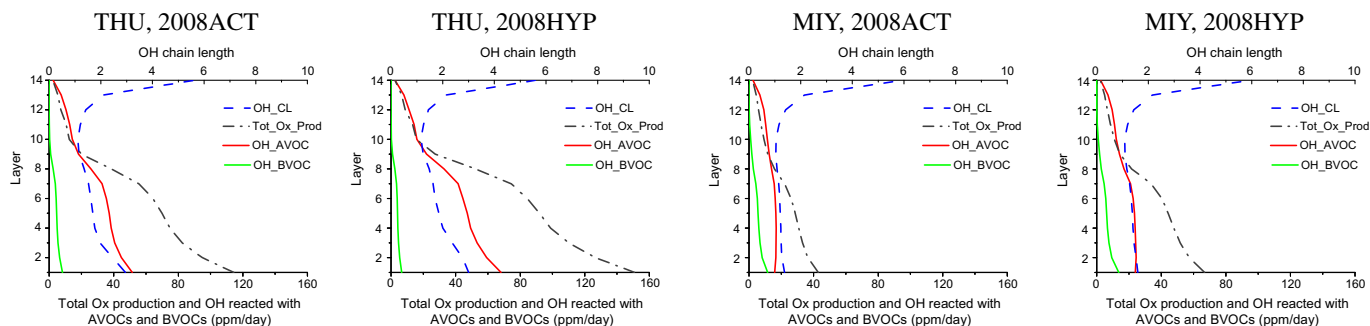
Fig. 8. Monthly-average vertical profiles of total O_x production, OH chain length and OH reacted with AVOCs and BVOCs and their responses to emission increases. (unit: ppm day^{-1}).

3.2.2. IPR analysis on PM$_{2.5}$ in August 2008

At both sites, PM processes are the dominant source for PM$_{2.5}$ in the PBL, while horizontal transport and cloud processes act as sinks of PM$_{2.5}$, as shown in Fig. 6a. Vertical profile of process contributions is shown in Fig. 6b. PM processes act as a source above layer 5 due to a dominance of the formation of SO$_4^{2-}$, NO$_3^-$, and SOA over other PM processes, while in low layers (layers 1—3), they act as a sink due to a dominance of the evaporation of NO$_3^-$ over other PM processes, that usually occurs during afternoon time, as shown in Fig. 6c. Emissions act as a major source for PM$_{2.5}$ at THU in surface layers (layers 1—2). In lower layers, vertical transport as the major sink transports particles to upper layers at THU. Emission contributes little to the PM production in the surface layer at MIY. The roles of vertical and horizontal transport are opposite at MIY and THU, due to different wind flow directions dominated by the profile of the vertical winds as discuss before. Differences between surface and upper-layer diurnal variations are apparent for both sites (see Fig. 6c and d). Besides the opposite roles of vertical and horizontal transport as discussed above, the diurnal contributions of PM processes are also different in surface and upper layers. In upper layers, PM processes act as a major source throughout the day, especially during afternoon time when the atmospheric oxidation capacity is strong and favors SO$_4^{2-}$, NO$_3^-$ and SOA formation. While in surface layers, PM processes act as a source in the nighttime but

a sink in the afternoon time, since the evaporation of NO$_3^-$ overwhelms the contributions from the formation of SO$_4^{2-}$ and SOA. A detailed discussion on each PM component, as SO$_4^{2-}$, NO$_3^-$, and SOA are provided in the Supplementary information.

In the PBL, contributions of emissions at THU and PM processes at both sites become larger in 2008HYP, along with stronger removal of horizontal transport (Fig. 6e). For PM$_{2.5}$, at THU, larger contributions by emissions occur in layers 1—2, along with a stronger vertical transport to upper layers, and a stronger horizontal transport to export PM$_{2.5}$ out of upper layers 7—9 (Fig. 6f-1). At MIY, the contribution from PM processes is increased in all layers within the PBL, along with a stronger horizontal and vertical transport (Fig. 6f-2). PM$_{2.5}$ concentrations are increased appreciably at both sites, especially during nighttime in the surface layer at THU (Figs. 6g-1), because of the weaker vertical mixing during nighttime and increases in NO$_3^-$ and SOA formation at night. At both sites, the net increase results in one obvious trough during 8—10 am (when the inversion layer breaks down) and one obvious peak during 6—8 am (when morning inversion layer is formed) at surface. One peak in layer 7 at both sites is at 10 am—12 pm and another at MIY appears at 2—3 pm (Fig. 6h), indicating that the PM processes start to contribute to PM$_{2.5}$ productions. The enhanced emissions in 2008HYP amplify the magnitudes of peak and trough PM$_{2.5}$, as shown in Fig. 6g and h.

3.2.3. Comparison of IPRs under two meteorological conditions

As discussed in Section 3.1, the MET-driven changes in 2008 relative to 2007 have a positive impact on the reductions of O$_3$
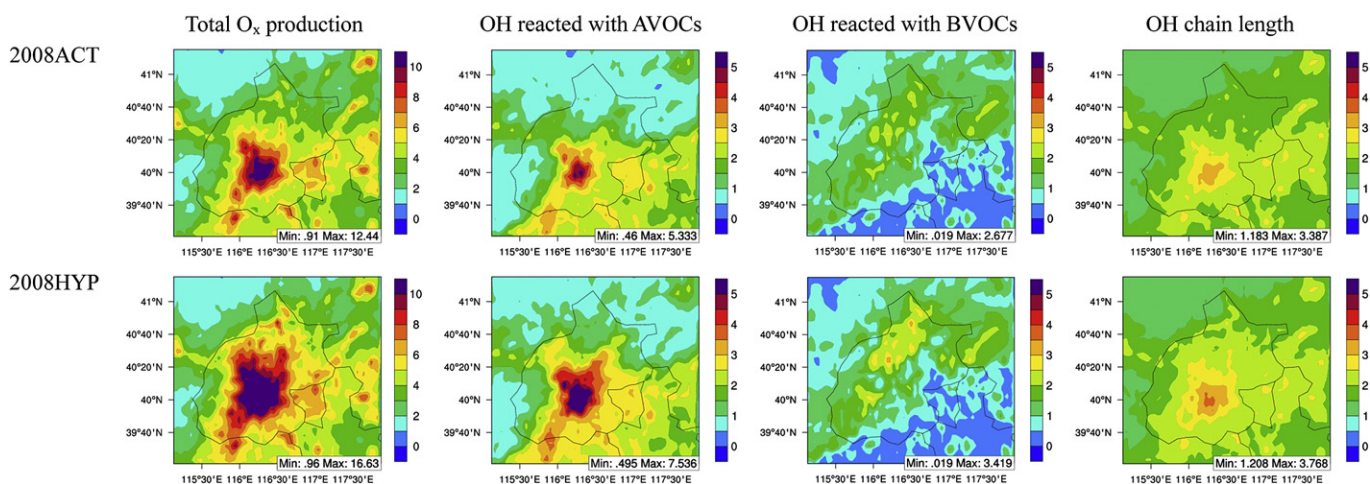

Fig. 9. Spatial distributions of total O_x production, OH chain length and OH reacted with AVOCs and BVOCs at surface in different emission scenarios. (unit: ppm h^{-1}).
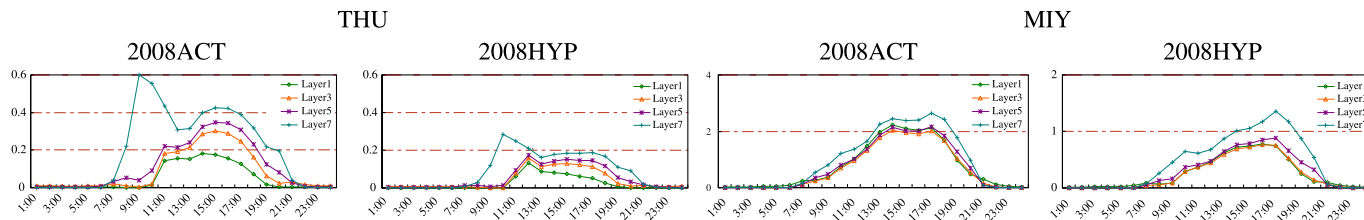
Fig. 10. Daily variation of $P_{H_2O_2}/P_{HNO_3}$ in different layers and its responses to emission increases (The height of layers 1, 3, 5, 7 above ground are 36, 145, 444, and 1070 m, respectively).

mixing ratios but a negative impact on reductions of $PM_{2.5}$ concentrations. The discrepancies of IPRs under the two meteorological conditions can help identify the dominant contributors provided by the meteorological influences. Fig. 7 shows the vertical profile of the responses of process contributions to different meteorological conditions which are obtained by taking differences in IPR results between simulations 2007HYP and 2008ACT at THU and MIY. A positive response indicates that such a process benefits for O_3 reduction (a weaker source or a stronger sink, depending on its role) in 2008, as compared with 2007, and a negative response indicates that such a process contributes more to O_3 in 2008. The differences in the vertical profiles of the vertical wind speed from both simulations at both sites are also shown to illustrate their impacts on dominant processes in each layer.

Compared to 2007ACT, weaker vertical winds from layers 1–7 at THU in 2008 indicate weaker vertical advection, which is the major sink in those layers for most of species, except in O_3 (in layer 1) and NO_3^- where the vertical turbulence is more important than advection. Fewer pollutants are brought by weaker upward winds from lower layers (1–7) to upper layers (8–9) where they are exported by horizontal transport. Such weaker exports do not benefit reductions of all pollutants at THU. Vertical winds at MIY within the PBL are similar (slightly stronger in 2007) in the two simulations. For O_3 in August 2008, less intensive photochemical reactions (as a source) to produce O_3 within the PBL and stronger dry deposition (as a sink) to reduce O_3 at surface benefit O_3 reduction. For fine particles in August 2008, stronger process contributions of cloud processes benefit the reductions of $PM_{2.5}$, NO_3^-, and SOA (as a sink), but enhance surface SO_4^{2-} concentrations (as a source). Slightly stronger dry deposition (as a sink) benefits SO_4^{2-} reduction. Smaller process contributions of PM processes benefit SOA and SO_4^{2-} reduction (as a source) but enhance NO_3^- and $PM_{2.5}$ concentrations in lower layers (1–6) (as a sink due to the evaporation of NO_3^-).

3.3. Analyses of Integrated Reaction Rates (IRR)

3.3.1. Total Ox production and OH chain length

Vertical profile of total Ox production (Total_OxProd) is given in Fig. 8. At THU, a large amount of Ox exists in lower layers, and its amount declines as altitude increases. The surface OH chain (OH_CL) is about 3 near surface, but decreases to <1 in upper layers till layer 11, they then increase again to almost 6 in layers 12–14. Total Ox production at MIY is much smaller (by ∼60%) than that at THU. The OH chain length is smaller than 1, with little changes aloft in layers 1–11, then increases to almost 6 in layers 12–14. The amount of OH reacted with anthropogenic VOCs (OH_AVOC) is larger than that with the biogenic VOCs (OH_BVOC), even at the rural site MIY, although the ratio of BVOC to total VOCs at MIY is larger than that at THU.

In the 2008HYP scenario, the total Ox production increases obviously by 30% in lower layers, the OH_AVOC also increases by 40% due to increased atmospheric oxidation capacity and AVOC emissions. OH_BVOC shows a slight increase at MIY due to increased atmospheric oxidation capacity.

Fig. 9 shows the spatial distributions of total O_x production, OH chain length and OH reacted with AVOCs and BVOCs at surface from simulations under the two different scenarios in 2008. Production of Total Ox and the amount of OH_AVOC are higher and the OH chain length is longer in urban areas than in rural areas for both simulations. OH_BVOC is generally higher in the north-west of Beijing areas than the remaining areas for both simulations, due to more forest there. Meteorological condition in 2008 benefits for the reduction of the overall tropospheric oxidation capacity, compared to that in 2007.

3.3.2. Indicators of NOx-/VOC-sensitive O_3 chemistry

Ratio of $P_{H_2O_2}/P_{HNO_3}$ is a useful indicator for NO_x- or VOC-limited O_3 photochemistry. Transition values of <0.2 and >0.2, correspond to VOC-limited, and NO_x-limited regimes, respectively (Sillman, 1995; Zhang et al., 2009). Daily variation of $P_{H_2O_2}/P_{HNO_3}$ in
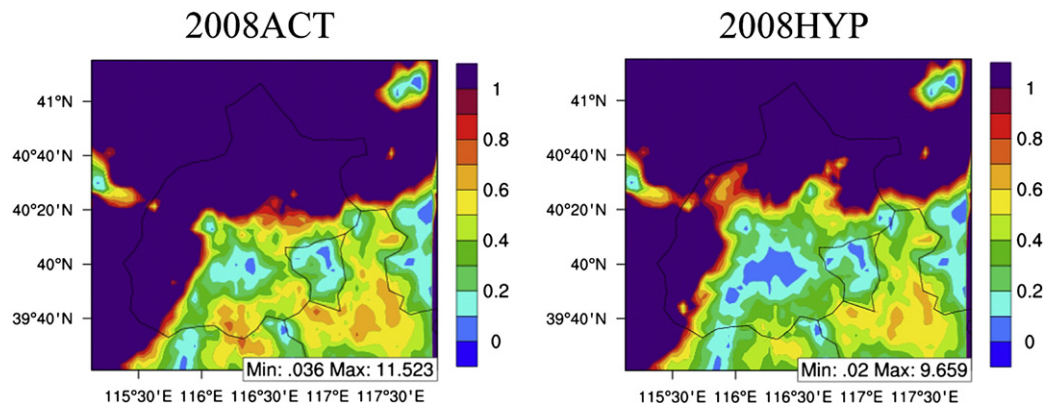

Fig. 11. Spatial distributions of monthly-mean ratios of surface $P_{H_2O_2}/P_{HNO_3}$ during afternoon hours (12:00–17:00, local time) in August 2008.

different layers (layers 1, 3, 5, 7) is given in Fig. 10. Higher ratio of $P_{H_2O_2}/P_{HNO_3}$ is found during afternoon hours when the photo-chemical reaction rates are high. In 2008ACT, surface $P_{H_2O_2}/P_{HNO_3}$ ratios at THU are slightly below 0.2 in the afternoon, indicating a ridgeline (sensitive to both NO_x and VOCs but more to NO_x) regime, but the ratios in upper layers are higher than 0.2, indicating a transition from ridgeline to NO_x-limited condition. O_3 chemistry at MIY is strongly NO_x-limited during the daytime.

Compared to 2008ACT, the ratios of $P_{H_2O_2}/P_{HNO_3}$ decrease at both sites from the simulation 2008HYP as shown in Fig. 10. THU site falls into the ridgeline (sensitive to both NO_x and VOCs but more to VOCs) regime with the ratio less than 0.1 at surface and also in upper layers (e.g., layers 3 and 5) except for layer 7. This means, control actions enforced during the 2008 Olympics with ~50% reduction of local NO_x and AVOCs emissions has changed O_3 chemical regime from the near VOC-limited ridgeline to near NO_x-limited ridgeline regime at surface and from ridgeline to NO_x-limited at some layers (e.g., layers 3 and 5) at THU. The combined NO_x and VOC emission control has not influenced surface O_3 mixing ratios during afternoon at THU surface as shown in Fig. 5g-1. A possible reason may be that the control benefit from VOC reductions could be partially compensated by NO_x reduction in such an area where O_3 chemistry is in the ridgeline regime, leading to nearly constant O_3 mixing ratios. The negative effect of NO_x emission control, however, has been compensated. Therefore, additional stronger NO_x controls could be effective to O_3 reduction. Compared to 2008HYP, obvious reductions of O_3 mixing ratios in 2008ACT can be found at MIY (see Fig. 5-2), which are under dominant NO_x-limited regime. Higher ratios of $P_{H_2O_2}/P_{HNO_3}$ in 2008ACT indicate a stronger NO_x-limited O_3 chemistry.

Fig. 11 shows the spatial distribution of the monthly-mean ratios of surface $P_{H_2O_2}/P_{HNO_3}$. The areas under obvious ridgeline (sensitive to both NO_x and VOCs but more to VOCs, with ratio below 0.1) regime can be found in the center of Beijing in 2008HYP. Compared with 2008HYP, the VOC-limited area located in the center of Beijing becomes smaller in 2008ACT scenario with ~50% reduction of local NO_x and AVOCs emissions. That suggests urban sites which are located in a stronger VOC-limited area are much harder to control O_3 than rural sites. Partly controls on NO_x without VOC emission reductions will leads to O_3 enhancement. Therefore, a stronger NO_x emission control with synergistic controls on VOC emissions is necessary.

4. Conclusions

Based on the detailed emission control information during the 2008 Beijing Olympics period, this study simulated air quality under two emission scenarios and two meteorology scenarios. The air quality benefits from emission reductions and meteorological variations are assessed. The dominant processes contributing to O_3, $PM_{2.5}$, SO_4^{2-}, NO_3^-, and SOA at one urban (THU) and one rural (MIY) site are identified. Indicator as $P_{H_2O_2}/P_{HNO_3}$ has been used to examine the NO_x vs. VOC-limited O_3 chemistry in Beijing.

There are several limitations in this study. First, we assume that the results from the two simulations (e.g., 2008ACT and 2008HYP) are additive which may not be valid for a highly non-linear system. The interaction between the two factors of emissions and meteo-rology or among more factors may contribute to some extent, e.g., the behavior of emission reductions effectiveness may change under different meteorological conditions. Second, the model bias-es and errors in meteorology and chemical predictions may affect process analysis results. For example, the simulated change of $PM_{2.5}$ (−4%) is not as much as the observed one (−19%). Slightly under-estimation of RH (by 6–20%) may cause the underestimation (by 28%) of aqueous-phase oxidation of SO_2 to form SO_4^{2-}. Uncertainty

of spatial distributions of NH_3 emission may explain the moderately overestimation of ammonium (by 57%). Nevertheless, the results from this study provide useful insights into the estimation on the effects of emissions reductions and atypical meteorological condi-tions on air quality improvement and the governing processes, which reflect the impacts from variations of emissions and meteorological conditions. They indicate that the importance of emission controls despite of positive changes in meteorology. This is because emission controls benefit for all pollutants reductions, though the extent of effectiveness from emission reductions varies from locations to locations. By contrast, the effect of meteorology-driven changes on species concentrations can be either ways at different locations. In addition, the spatial and temporal distribu-tions of the differences of O_3 chemistry regimes should be considered in emission control policy-making process. A stronger NO_x control with synergistic controls on VOCs is essential to reduce O_3 concentrations in urban areas.

Appendix. Supplementary information

Supplementary information related to this article can be found at doi:10.1016/j.atmosenv.2011.01.025.

References

Binkowski, F.S., Roselle, S.J., 2003. Models-3 Community Multiscale Air Quality (CMAQ) model aerosol component, 1. Model description. Journal of Geophysical Research 108, 4183. doi:10.1029/2001JD001409.

Branis, M., Vetvicka, J., 2010. PM_{10}, ambient temperature and relative humidity during the XXIX summer Olympic games in Beijing: were the athletes at risk? Aerosol and Air Quality Research 10 (2), 102–110.

Cermak, J., Knutti, R., 2009. Beijing Olympics as an aerosol field experiment. Geophysical Research Letters 36, L10806. doi:10.1029/2009GL038572.

Duan, F.-K., He, K.-B., Ma, Y.-L., et al., 2006. Concentration and chemical charac-teristics of $PM_{2.5}$ in Beijing, China: 2001–2002. Science of the Total Environ-ment 355, 264–275.

Fu, J.S., Streets, D.G., Jang, C.J., et al., 2009. Modeling regional/urban ozone and particulate matter in Beijing, China. Journal of the Air & Waste Management Association 59.

Hao, J.-M., He, K.-B., Duan, L., et al., 2007. Air pollution and its control in China. Frontiers of Environmental Science and Engineering in China 1, 129–142.

He, K., Yang, F., Ma, Y., et al., 2001. The characteristics of $PM_{2.5}$ in Beijing, China. Atmospheric Environment 35, 4959–4970.

Jang, J.C., Jeffries, H.E., Tonnesen, S., 1995. Sensitivity of ozone to model grid reso-lution-II. Detailed process analysis for ozone chemistry. Atmospheric Environ-ment 29, 3101–3114.

Liu, X.-H., Zhang, Y., Cheng, S.-H., et al., 2010a. Understanding of regional air pollution over China using CMAQ − part I. Performance evaluation and seasonal variation. Atmospheric Environment 44 (20), 2415–2426.

Liu, X.-H., Zhang, Y., Xing, J., et al., 2010b. Understanding of regional air pollution over China using CMAQ − part II. Process analysis and ozone sensitivity to precursor emissions. Atmospheric Environment 44 (20), 3719–3727.

Liu, P., Zhang, Y., Yu, S., et al., 2011. Use of a process analysis tool for diagnostic study on fine particulate matter predictions in the U.S. Part II: process analyses and sensitivity simulations. Atmospheric Pollution Research 2 (1), 61–71.

Mijling, B., van der A.R.J., Boersma, K.F., et al., 2009. Reductions of NO_2 detected from space during the 2008 Beijing Olympic Games. Geophysical Research Letters 36.

Sillman, S., 1995. The use of NOy, H_2O_2, and HNO_3 as indicators for ozo-ne−NO_x−hydrocarbon sensitivity in urban locations. Journal of Geophysical Research 100 (D7), 4175–4188.

Sun, Y.-L., Zhuang, G.-S., Wang, Y., et al., 2004. The air-borne particulate pollution in Beijing-concentration, composition, distribution and sources. Atmospheric Environment 38, 5991–6004.

Tang, G., Li, X., Wang, Y., et al., 2009. Surface ozone trend details and interpretations in Beijing, 2001–2006. Atmospheric Chemistry and Physics 9, 8813–8823.

Tonse, S.R., Brown, N.J., Harley, R.A., et al., 2008. A process-analysis based study of the ozone weekend effect. Atmospheric Environment 42, 7728–7736.

Wang, T., Xie, S.-D., 2009. Assessment of traffic-related air pollution in the urban streets before and during the 2008 Beijing Olympic Games traffic control period. Atmospheric Environment 43, 5682–5690.

Wang, T., Ding, A., Gao, J., et al., 2006. Strong ozone production in urban plumes from Beijing, China. Geophysical Research Letters 33, L21806. doi:10.1029/2006GL027689.

Wang, K., Zhang, Y., Jang, C.J., et al., 2009a. Modeling study of intercontinental air pollution transport over the trans-Pacific region in 2001 using the Community Multiscale Air Quality (CMAQ) modeling system. Journal of Geophysical Research 114, D04307. doi:10.1029/2008JD010807.

Wang, W.-T., Primbs, T., Tao, S., et al., 2009b. Atmospheric particulate matter pollution during the 2008 Beijing Olympics. Environmental Science & Technology 43, 5314–5320.

Wang, X., Westerdahl, D., Chen, L.-C., et al., 2009c. Evaluating the air quality impacts of the 2008 Beijing Olympic Games: on-road emission factors and black carbon profiles. Atmospheric Environment 43, 4535.

Wang, Y.-X., Hao, J.-M., McElroy, M.B., et al., 2009d. Ozone air quality during the 2008 Beijing Olympics: effectiveness of emission restrictions. Atmospheric Chemistry and Physics 9, 5237–5251.

Wang, S.-X., Zhao, M., Xing, J., et al., 2010a. Quantifying the air pollutants emission reduction during the 2008 Olympic games in Beijing. Environmental Science & Technology 44, 2490–2496.

Wang, T., Nie, W., Gao, J., et al., 2010b. Air quality during the 2008 Beijing Olympics: secondary pollutants and regional impact. Atmospheric Chemistry and Physics 10, 7603–7615.

Witte, J.C., Schoeberl, M.R., Douglass, A.R., et al., 2009. Satellite observations of changes in air quality during the 2008 Beijing Olympics and Paralympics. Geophysical Research Letters 36, L17803. doi:10.1029/2009GL039236.

Xu, J., Zhang, Y.-H., Fu, J.S., et al., 2008. Process analysis of typical summertime ozone episodes over the Beijing area. Science of the Total Environment 399, 147–157.

Yu, H., Wang, P.-C., Zong, X.-M., et al., 2010. Change of NO_2 column density over Beijing from satellite measurement during the Beijing 2008 Olympic Games. Chinese Science Bulletin 55 (3).

Zhang, Y., Vijayaraghavan, K., Seigneur, C., 2005. Evaluation of three probing techniques in a three-dimensional air quality model. Journal of Geophysical Research 110, D02305. doi:10.1029/2004JD005248.

Zhang, Y., Wen, X.-Y., Wang, K., et al., 2009. Probing into regional O_3 and PM pollution in the U.S., part II. An examination of formation mechanisms through a process analysis technique and sensitivity study. Journal of Geophysical Research 114, D22305. doi:10.1029/2009JD011900.

Zhang, Y., Liu, P., Liu, X.-H., et al., 2010. A Comparative study of homogeneous nucleation parameterizations, part II. 3-D model application and evaluation. Journal of Geophysical Research 115, D20213. doi:10.1029/2010JD014151.

Zhao, X.-J., Zhang, X.-L., Xu, X.-F., et al., 2009. Seasonal and diurnal variations of ambient $PM_{2.5}$ concentration in urban and rural environments in Beijing. Atmospheric Environment 43, 2893–2900.

Zheng, M., Salmon, L.G., Schauer, J.J., et al., 2005. Seasonal trends in $PM_{2.5}$ source contributions in Beijing, China. Atmospheric Environment 39, 3967–3976.